ACCURACY IMPROVEMENT OF FISHEYE STEREO CAMERA BY COMBINING MULTIPLE DISPARITY OFFSET MAPS

Jiayi Ling[1], Tomoyuu Sakuda[1], Hirotaka Iida[1], Yonghoon Ji[1], Kazunori Umeda[1], Akira Ohashi[2], Daisuke Fukuda[2], Shuzo Kaneko[2], and Junya Murayama[2]

***Abstract*— This paper proposes a novel method that significantly improves the accuracy of the fisheye stereo camera using multiple disparity offset maps that contain disparity error information. The disparity offset map is constructed based on disparity errors that are calculated from the feature points extracted from an object with a known distance. Modified stereo matching process based on the maps is carried out to greatly reduce the disparity errors that cannot be completely removed by general calibration scheme. Furthermore, the our method is possible to achieve high accuracy in both short and long range by combining the multiple maps. The proposed method is verified by experiments.**

I. INTRODUCTION

In recent years, cameras and range sensors for driving assistance of automobiles are often used, and are becoming capable of dealing with various situations. Among them, this paper focus on the fisheye camera, since it has a wide viewing angle of about $180°$ and the construction of a fisheye stereo camera using two fisheye cameras makes it possible to measure a wide dense range image. Several studies on fisheye stereo cameras have been intensively conducted. Abraham et al. simplified stereo matching process by rectifying the images from the fisheye stereo camera [1]. Moreau et al. presented the epipolar constraint of a fisheye image for an equisolid angle projection model [2]. In some studies, a fisheye stereo camera was applied to a UAV (unmanned aerial vehicle) [3] and vehicles [4], [5], [6]. In these studies, fisheye images were usually transformed to perspective images to simplify the corresponding point search of stereo images. On the other hand, Ohashi et al. realized the reduction of fisheye image distortion and simplification of corresponding point search by equirectangular projection [7], [8]. However, there is a limit to distance measurement accuracy due to large distortion compared to perspective projection images and errors in extrinsic parameters. Yamano et al. improved the accuracy by using a disparity offset map that corrects the disparity only for the long-range target at a known distance [9]. However, due to the anisotropy of the distortion of the fisheye image, the accuracy of the range image strongly depends on the distance of the object. In general, the effect of anisotropy increases with distance from the reference position where the disparity offset map is generated. To overcome the limitation above, we propose a method to generate a short-distance disparity offset map using our newly constructed short-range calibration target. In addition, we aim to improve the accuracy of fisheye stereo cameras by combining short-range and long-range disparity offset maps.

[1]The Course of Precision Engineering, School of Science and Engineering, Chuo University, 1-13-27 Kasuga, Bunkyo-ku, Tokyo, Japan sakuda@sensor.mech.chuo-u.ac.jp

[2] Clarion, 7-2 Shintoshin, Chuo-ku, Saitama-shi, Saitama, Japan

II. ACCURACY IMPROVEMENT USING DISPARITY OFFSET MAP

A. Generation of Short-Range Disparity Offset Map

The disparity offset map represents the disparity errors of all pixels with respect to a certain distance from the origin of the fisheye stereo camera (i.e., the lens center of the right camera). In order to generate a short-range disparity offset map, we constructed a new calibration target with a radius of 1 m that can virtually simulate a hemisphere by rotating the camera around the origin as shown in Fig. 1. Inside the target, round patterns with colors are attached repeatedly that makes it easy to capture features. The procedure for feature point matching is shown in Fig. 2. First, the color of the circular pattern with a diameter of 3 cm on the target is detected from the captured left and right images. Next, the each center of each detected area is calculated. Then, matching process is performed using only the calculated center of the circular pattern as a feature point. Finally, we can generate a short-range disparity offset map from the disparity errors of feature points.

B. Combination of Disparity Offset Maps

By combining the disparity offset maps, the disparity k between corresponding points of the left and right images is corrected by a linear equation. The corrected disparity k' is calculated as follows:

$$k' = ak + b. \tag{1}$$

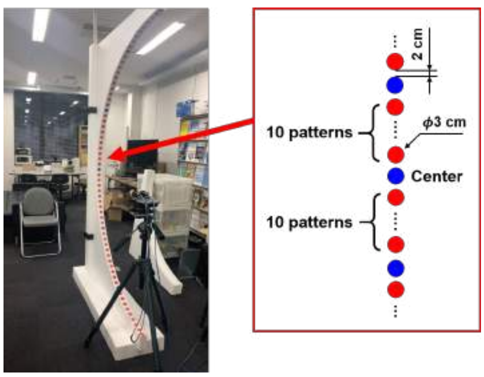

Fig. 1. Short-range calibration target.

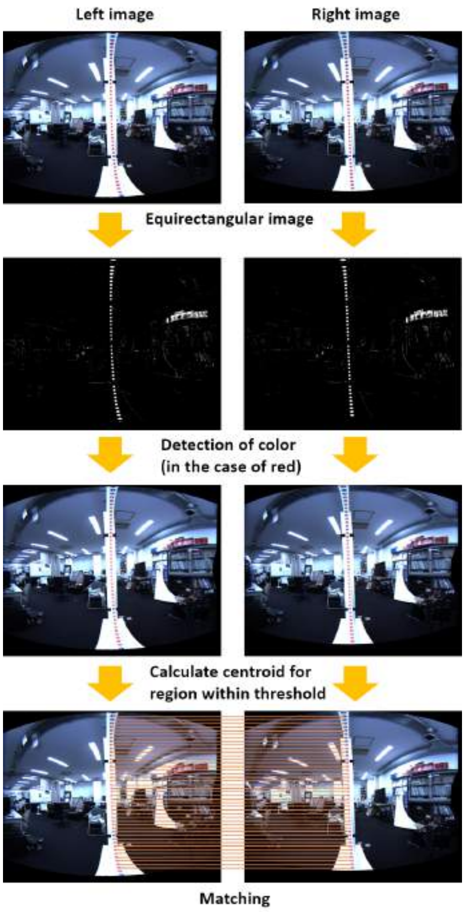

Fig. 2. Procedure of feature point matching.

The correction coefficients a and b for each pixel can be obtained by the following procedure:

1) The true values of the disparities in the u (horizontal) and v (vertical) directions with respect to the long-range target of the pixel (u, v) in the equirectangular image of resolution $M \times N$ are defined as k^0_{Fu} and k^0_{Fv}. In the same way, the true values of the disparities in the u and v directions with respect to the short-range target are defined as k^0_{Nu} and k^0_{Nv}. These variables are calculated as follows:

$$\lambda = \frac{\pi}{M}(u - \frac{M}{2}), \tag{2}$$

$$\phi = \frac{\pi}{M}(v - \frac{N}{2}), \tag{3}$$

$$\tan\phi_0 = \frac{\tan\phi}{\cos\lambda}, \tag{4}$$

$$k^0_u = \tan^{-1}(\frac{b\sin\frac{\pi u}{M}}{D_T\cos\phi - b\cos\frac{\pi u}{M}}) \times \frac{M}{\pi}, \tag{5}$$

$$k^0_v = \tan^{-1}(\tan\phi_0\cos(\lambda + \frac{\pi k^0_u}{M})) \times \frac{M}{\pi} + \frac{N}{2} - v, \tag{6}$$

where λ and ϕ are the azimuth and elevation angles to the target, respectively. ϕ_0 is the elevation angle when the azimuth angle is zero. b and D_T denote the length of the baseline and the known distance, respectively. k^0_u and k^0_v are the true values of the disparity in the u and v directions. Here, we set D_T to 300 m and 1 m to obtain the true value of the long-range and short-range disparities, respectively.

2) Let the disparity errors in the u and v directions in the long-range disparity offset map of the pixel (u, v) be e_{Fu} and e_{Fv}. In the same way, let e_{Nu} and e_{Nv} be the disparity errors in the u and v directions in the short-range disparity offset map. Based on these, the actual disparities k_{Fu} and k_{Fv} in the long range and the actual disparities k_{Nu} and k_{Nv} in the short range are calculated as follows:

$$k_{Fu} = k^0_{Fu} + e_{Fu}, \tag{7}$$

$$k_{Fv} = k^0_{Fv} + e_{Fv}, \tag{8}$$

$$k_{Nu} = k^0_{Nu} + e_{Nu}, \tag{9}$$

$$k_{Nv} = k^0_{Nv} + e_{Nv}. \tag{10}$$

3) Correction coefficients a and b are calculated as follows:

$$a_u = \frac{k^0_{Fu} - k^0_{Nu}}{k_{Fu} - k_{Nu}}, \tag{11}$$

$$b_u = k^0_{Nu} - a_u k_{Nu}, \tag{12}$$

$$a_v = \frac{k^0_{Fv} - k^0_{Nv}}{k_{Fv} - k_{Nv}}, \tag{13}$$

$$b_v = k^0_{Nv} - a_v k_{Nv}, \tag{14}$$

The disparity k_u in the u direction is calculated by template matching between the corresponding points of the left and right images. The disparity k_v in the v direction is obtained by substituting k_u into (6). Finally the disparities after correction k'_u and k'_v can be calculated as follows:

$$k'_u = a_u k_u + b_u, \tag{15}$$

$$k'_v = a_v k_v + b_v. \tag{16}$$

III. EXPERIMENTS

Figure 3 shows the fisheye stereo camera used for our experiments. The cameras used in the experiment were FLIR Flea3 equipped with a fisheye lens, SPACE TV1634M. The intrinsic parameters of the fisheye lens were estimated using the OcamCalib Toolbox for MATLAB [10]. The resolution of both cameras was 1,328 $\times$ 1,048 pixels, and their baseline was 52 mm. The angle of view was $165°$ in the horizontal direction and $132°$ in the vertical direction. To reflect the short-range calibration target with a radius of 1 m in all areas of the image (i.e., simulation of the semicircular surface), as shown in Fig. 4, 175 images were taken by rotating the stereo camera slightly around the Y-axis of the camera coordinate system as shown in the right side of the same figure. Here, five blue patterns and other red patterns are attached to the target. Table I shows the detection conditions for red and blue patterns in HSV color space. The values of the conditions are ± 20 of the maximum and minimum value of the color

TABLE I

COLOR DETECTION CONDITIONS IN HSV COLOR SPACE.

/	Hue	Saturation	Value
Red	120-180	80-185	more than 80
Blue	80-140	140-255	more than 120

TABLE II

CONDITIONS TO CALCULATE CENTER OF EACH DETECTED AREA.

/	Condition	Circularity	Area [$pixel^2$]
Red	/	more than 0.3	50-320
Blue	1	more than 0.5	50-150
Blue	2	0.4-0.6	180-300

in the patterns which are selected randomly. Table II shows the conditions to calculate the center of each detected area. For the blue pattern, different threshold values were applied according to whether they were near the center or borders because the circle is distorted depending on the position in the image as shown in Fig. 4. Figure 5 shows the short-range disparity offset map generated by the proposed method. Figure 6 shows the long-range disparity offset map generated by the previous work [9].

To verify the effectiveness of the proposed method, comparative experiments were conducted under the different conditions: without correction and correction using proposed method. We also measured targets made from black and white paper located at different distances: 1 m, 3 m, and 5 m. Figure 7 shows the experimental environment and 17 measurement positions with different azimuth and elevation angles in the range image where the evaluation was carried out. Here, each color corresponds to colors in Figs. 9, 10, and 11. The generated range images are shown in Fig. 8. The distance measurement results were evaluated by the mean error and its standard deviation as shown in Figs. 9, 10, and 11. They were evaluated by the mean and standard deviation of 25 points acquired near the measurement point. In case of the 1 m measurement results (Fig. 9), the distance accuracy was high with and without correction. In case of the 3 m and 5 m measurement results (Figs. 10 and 11), the errors of $\{-60°, -45°\}$ positions were large even when they were corrected. Overall, the proposed method mostly outputs the most accurate results; however, there were still some measurement errors. This is because the feature points from the long-range disparity offset map were sparse. Moreover, the feature points (i.e., center of the circular patterns) from the short-range disparity offset map cannot be extracted with high accuracy depending on the color detection conditions.

IV. CONCLUSIONS

In this paper, we proposed a method to generate a short-range disparity offset map using color information for the constructed short-range calibration target in order to improve the accuracy of fisheye stereo camera. The accuracy of the fisheye stereo camera was improved by combining multiple disparity offset maps. The future work related to this study is as follows. We will examine a method that can extract

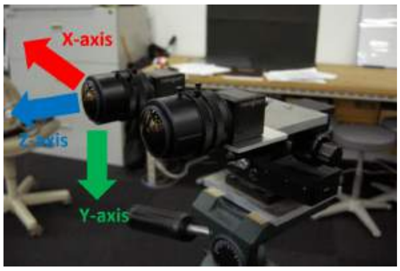

Fig. 3. Fisheye stereo camera.

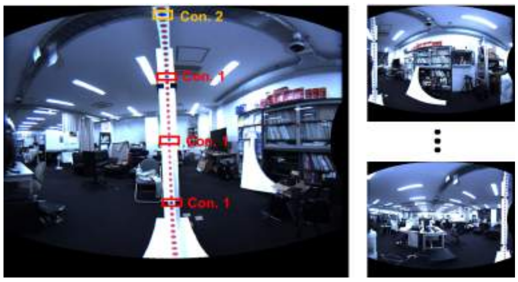

Fig. 4. Conditions to calculate center of blue pattern.

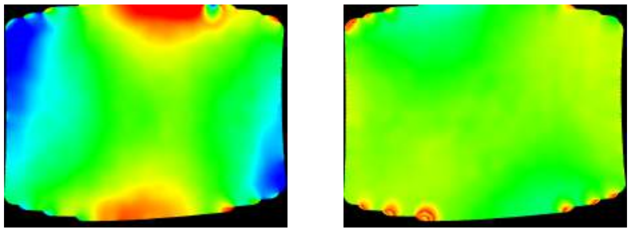

(a) (b)

Fig. 5. Short-range disparity offset maps: (a) u direction and (b) v direction. Color represents disparity values from -2 pixel (red) to 2 pixel (blue).

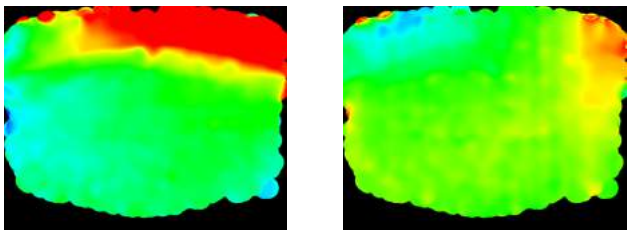

(a) (b)

Fig. 6. Long-range disparity offset maps: (a) u direction and (b) v direction. Color represents disparity values from -2 pixel (red) to 2 pixel (blue).

dense feature points of long-range targets. In addition, we plan to improve the feature point acquisition method, such as automating color detection of the patterns on short-range targets and improving the measurement accuracy of the center position of the patterns.

REFERENCES

[1] S. Abraham and W. Forstner, “Fish-eye stereo calibration and epipolar rectification,” *Journal of Photogrammetry and Remote Sensing*, vol. 59, no. 5, pp. 278-288, 2005.

[2] J. Moreau, S. Ambellouis, and Y. Ruichek, “Equisolid fisheye stereovision calibration and point cloud computation,” in *Proceedings of*

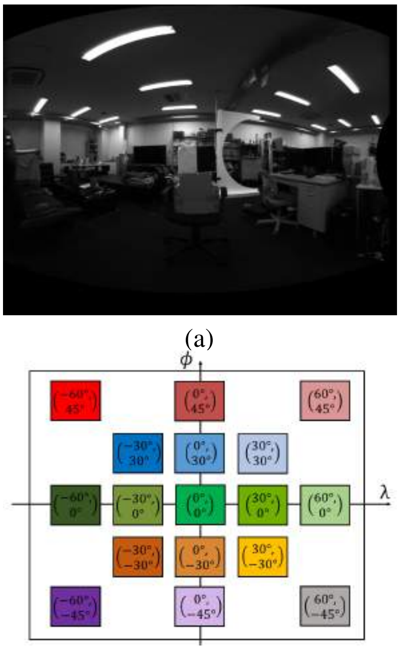

(a)

(b)

Fig. 7. Experimental conditions: (a) indoor environment and (b) measurement points.

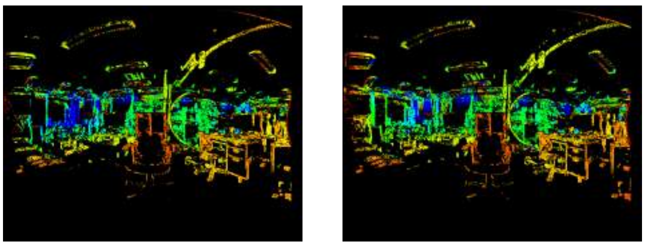

(a)

(b)

Fig. 8. Range images: (a) without correction and (b) with correction by multiple disparity offset maps. Color represents distance values from 0 m (red) to 10 m (blue).

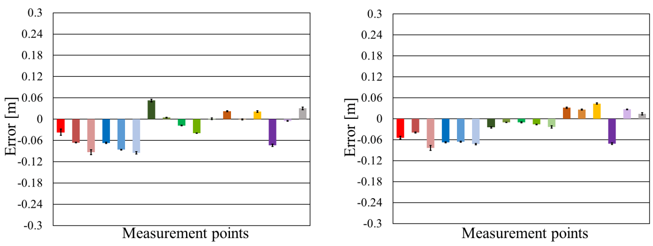

(a)

(b)

Fig. 9. Mean and standard deviation of errors at distance of 1 m: (a) without correction and (b) with correction by multiple disparity offset maps.

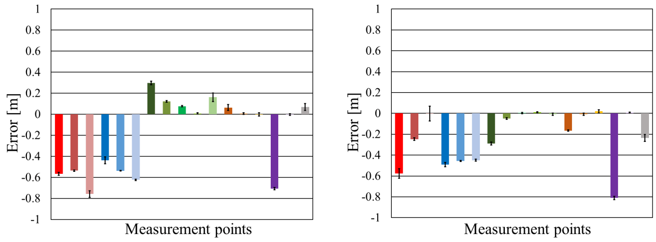

(a)

(b)

Fig. 10. Mean and standard deviation of errors at distance of 3 m: (a) without correction and (b) with correction by multiple disparity offset maps.

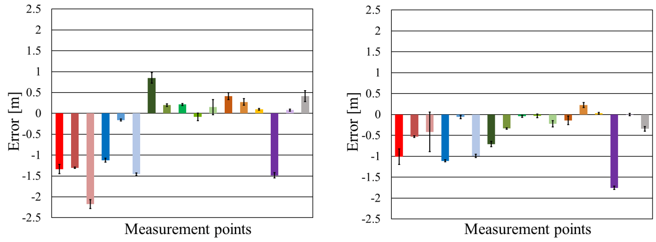

(a)

(b)

Fig. 11. Mean and standard deviation of errors at distance of 5 m: (a) without correction and (b) with correction by multiple disparity offset maps.

International Archives of the Photogrammetry, Remote Sensing and Spatial Information Sciences, pp. 167-172, 2013.

[3] N. Krombach, D. Droeschel, and S. Behnke, "Evaluation of stereo algorithms for obstacle detection with fisheye lenses," in *Proceedings of International Archives of the Photogrammetry, Remote Sensing and Spatial Information Sciences*, pp. 33-40, 2015.

[4] P. Furgale et al., "Toward automated driving in cities using close-tomarket sensors: An overview of the V-Charge Project," in *Proceedings of IEEE Intelligent Vehicles Symposium (IV)*, pp. 809-816, 2013.

[5] S. K. Gehrig, "Large-field-of-view stereo for automotive applications," in *Proceedings of Workshop on Omnidirectional Vision, Camera Networks and Non-classical cameras*, 2005.

[6] D. Kim, J. Choi, H. Yoo, U. Yang, and K. Sohn "Rear obstacle detection system with fisheye stereo camera using HCT," *Expert Systems With Applications*, vol. 42, pp. 6295-6305, 2015.

[7] A. Ohashi, Y. Tanaka, G. Masuyama, K. Umeda, D. Fukuda, T. Ogata, T. Narita, S. Kaneko, Y. Uchida, and K. Irie "Fisheye stereo camera using equirectangular images," in *Proceedings of the 2016 11th France-Japan Congress on Mechatronics 9th Europe-Asia Congress on Mechatronics 17th International Conference on Research and Education in Mechatronics*, pp. 284-289, 2016.

[8] A. Ohashi, F. Yamano, G. Masuyama, K. Umeda, D. Fukuda, K. Irie, S. Kaneko, J. Murayama, and Y. Uchida, "Stereo rectification for equirectangular images," in *Proceedings of the 2017 IEEE/SICE International Symposium on System Integration*, 2017.

[9] F. Yamano, H. Iida, K. Umeda, A. Ohashi, D. Fukuda, S. Kaneko, J. Murayama, and Y. Uchida, "Improving the accuracy of a fisheye stereo camera with a disparity offset map," in *Proceedings of the 12th France-Japan and 10th Europe-Asia Congress on Mechatronics*, pp. 88-91, 2018.

[10] D. Scaramuzza, A. Martinelli, and R. Sliegwart, "A toolbox for easily calibrating omnidirectional cameras," in *Proceedings of the 2006 IEEE/RSJ International Conference on Intelligent Robots and Systems*, pp. 5695-5701, 2006.